UV/Thermally Curable, Soy Protein-based Resin as a Versatile Platform for Chemical Delivery

Long Jiang, Qian Ma
North Dakota State University

Introduction

Pesticides and fertilizers have played pivotal roles in modern agriculture and horticulture, bringing significant agronomic and economic benefits to the world. However, their widespread and excessive use also poses environmental risks and causes waste of resources/energy due to substantial losses of the chemicals to the environment. Using controlled-release pesticides/fertilizers can alleviate these problems but their substantially higher cost has restricted their use to high value crops, specific cultivation systems and non-agricultural sectors (professional horticulture, nurseries, greenhouses, golf courses, household consumers, turf, landscape gardeners and public parks).

The goal of this project is to develop a low-cost, environmentally friendly vehicle to efficiently deliver pesticides/fertilizer in a controlled manner that is tailored to plants' growth needs. UV/thermally curable, soy protein-based resin was investigated as the main material to produce the delivery vehicle in this research. Two curing methods, UV and thermal curing, were used to prepare two different delivery systems. Release behavior of the two systems with various formulations were studied. Both systems showed controlled release with the release rates varying with their formulations. Further investigations on the formulation and processing conditions are desired to obtain the optimum ones for field tests.

Materials and Methods

Synthesis of methacrylated soy protein isolate (MSPI) The synthesis of MSPI was performed though a two-step process including SPI dissolution and SPI methacrylation based on a previously reported study. Briefly, SPI was mixed with distilled water (15 wt %) in a round bottom flask. A KOH aqueous solution (8 wt %) was added to the SPI/water mixture in the flask to give a SPI/H_2O/KOH ratio of 1/7/0.09 (w/w/w) and a pH value of 11.6. The flask was then placed in a preheated oil bath at 70 °C and the mixture was magnetically stirred at 450 rpm for 1.5 h to complete the dissolution. The product was allowed to cool to room temperature naturally for about 30 min and centrifuged at 9000 rpm for 5 min to remove any undissolved SPI and impurities. In the second step, the alkali-treated SPI was reacted with methacrylic anhydride (MAh) to synthesize MSPI. MAh (14 wt % of SPI dry weight) was added into the SPI solution and stirred with a magnetic stirrer (500 rpm) at room temperature for 30 min to obtain MSPI. The final concentration of the obtained MSPI solution was 12.15 wt%.

Two controlled release systems based on MSPI were prepared in this project. One is fabricated through UV curing of MSPI and the other one is through thermal curing.

Preparation of UV-cured MSPI-based film MSPI solution, crosslinker (acrylated epoxidized soy bean oil (AESO) or poly(ethylene glycol) diacrylate (PEGDA) at 40 wt% MSPI), cellulose nanofibrils (CNF) (at 5 or 10 wt% MSPI), photo-initiator (PI) (2-Hydroxy-2-methylpropiophenone) (6 wt% of MSPI and crosslinker), and aspirin (as a model drug) were mixed together. The mixture was poured into a polypropylene Petri dish and allowed to dry under ambient conditions for 2 days. The obtained film (thickness ~ 0.4 mm) was then crosslinked under a UV lamp (365 nm/250 W, 20 cm distance between the lamp and the sample). In total, films with four different formulations were prepared.

Preparation of bacterial cellulose (BC)/MSPI gels by thermal curing Bacterial cellulose (BC) is produced by some bacteria and the material has a natural cellulose fiber network structure. BC was added into MSPI in this part of study to strengthen MSPI gel. The obtained 12.15 wt% MSPI solution was diluted with deionized water to concentrations of 4.15, 8.15, 10, and 12.15 wt%. Tert-Butyl peroxybenzoate (thermal initiator) was added at 2% (w/w) of MSPI and mixed well in the solution using an IKA T25 digital ultra-turrax homogenizer at 4000 rpm for 15 min. Wet BC cubes were pressed to a thickness of 1mm by placing between 2 aluminum plates with spacers to remove their absorbed water. The compressed BC cubes were then

immersed in a 20 ml MSPI solution and stirred at 200 rpm and 20 °C for 2 days to allow complete impregnation by the solution. The compressed cubes almost completely recovered their original size and shape. The BC/MSPI were cured in an oven at 100 °C for 6 h. The obtained BC/MSPI composite hydrogels were washed with deionized water to remove unreacted reagents on the surface and freeze-dried at -50 °C for 48 h for characterizations and measurements. The preparation of fertilizer-containing hydrogel BC/MSPI-$(NH_4)_2SO_4$ followed the same procedure except that $(NH_4)_2SO_4$ was mixed with the diluted MSPI solution before the impregnation of the compressed BC cubes. The thermally cured BC/MSPI-$(NH_4)_2SO_4$ composite hydrogels were also washed with deionized water to remove unreacted reagents and attached fertilizers on the surface and freeze-dried for fertilizer release test in water.

^{1}H NMR characterization The functionalization and crosslinking reactions were characterized using proton nuclear magnetic resonance spectroscopy (^{1}H NMR). ^{1}H NMR analysis was performed on an ECA Series 400 MHz NMR spectrometer (JEOL, Japan). Samples were dissolved in Deuterium oxide (D_2O) at 10 mg/ml and the spectra were recorded.

SEM characterization The cross-sectional morphology of BC/MSPI composite hydrogels was studied using a field-emission scanning electron microscope (SEM, JSM-7600F, JEOL, Japan) at an accelerating voltage of 5 kV. The freeze-dried samples were fractured and coated with gold for observation.

Mechanical properties of BC/MSPI composite hydrogels Compression tests of the BC/MSPI hydrogels were performed using an MTS's Insight Electromechnical 5kN Extended Length Testing System. Cubic samples were tested at a constant speed of 3 mm/min and compressed up to 90% strain. At least three specimens were tested for each sample.

Swelling and dissolution of BC/MSPI composite hydrogels in water Swelling and dissolution studies were conducted by immersing freeze-dried composite hydrogels into 50 ml deionized water under gentle stirring for 5 days. The samples were removed from water at predetermined time intervals, dabbed with tissue to remove surface water, and measured using a microscale. This process was repeated until absorption/swelling equilibrium was reached when the weight of the hydrogels was constant. The swelling rate (SR) of the samples was calculated according to the equation: $\text{Swelling Rate}(\%) = (W_t - W_0)/W_0$, where W_0 was the weight of dried hydrogels and W_t was the weight of the swollen hydrogels at time *t*. The fully swollen hydrogels were dried in an oven at 100 °C for 24h until a constant weight was reached. The solubility of the samples was obtained according to the equation: $S\text{olubility}(\%) = (W_0 - W_r)/W_0$, where W_0 was the initial weight of dried hydrogels and W_r was the residual weight of hydrogels after drying.

Controlled release of $(NH_4)_2SO_4$ fertilizer from BC/MSPI-$(NH_4)_2SO_4$ in water In order to understand the release of $(NH_4)_2SO_4$ fertilizer from BC/MSPI, the freeze-dried BC/MSPI-$(NH_4)_2SO_4$ was immersed in 25 ml deionized water and the conductivity of the water was measured at predetermined time intervals. The conductivity is proportional to the concentration of total electrolytes in the solution. The experiments were carried out at 25 °C under gentle magnetic stirring.

Results and Discussion

UV-cured MSPI system

Methacrylation of SPI and UV crosslinking of MSPI based films were confirmed by the FTIR results. In Figure 1a, alkaline treated SPI showed characteristic amide bands at 1657, 1527, 1391, and 1231 cm^{-1} assigned to amide I (C=O stretching), amide II (N–H bending), and amide III (C–N and N–H stretching), respectively. After the methacrylation, two new peaks appeared in the MSPI sample at 1130 cm^{-1} and 930 cm^{-1} (representing wagging and stretching of C-H of $RC=CH_2$, respectively). The signal from C=C of the methacrylate group was difficult to detect because it overlapped with the one from the amide I of SPI. Meanwhile, peaks at 1316 cm^{-1} and 1169 cm^{-1} of the MSPI sample became stronger than that of alkaline treated SPI due to C-CH_3 stretching and C-O stretching of the methacrylate group, respectively. These results indicated successful grafting of the methacrylate group onto SPI.

Figure 1b show the spectra of the MSPI based films before and after UV crosslinking. The band at 1724 cm^{-1} of the uncured MSPI based film is attributed to C=O of the acrylate group of AESO. The band at 1635 cm^{-1} is attributed to the overlapping peaks from amide I and C=C of MSPI and the acrylate group of AESO. The band at 1405 cm^{-1} is attributed to the overlapping peaks from C-O-H group of MSPI and CNF and C=C of AESO. The band at 985 cm^{-1} is attributed to the overlapping peaks of C-O stretching of MSPI and CNF and C=C out of plane bending of the acrylate group of AESO, The band at 809 cm^{-1} is attributed to C=C out of plane bending of the acrylate group of AESO. In the cured MSPI based film, the intensity of the peaks at 1635, 1405, 985, 809 cm^{-1} decreased significantly due to the consumption of the C=C bonds of the acrylate and methacrylate moieties. Moreover, the C=O stretching shifted to a higher frequency at 1737 cm^{-1} due to the diminishing conjugation between C=O and C=C caused by the disappearance of C=C stretching. These results clearly confirmed the complete consumption of C=C bonds.

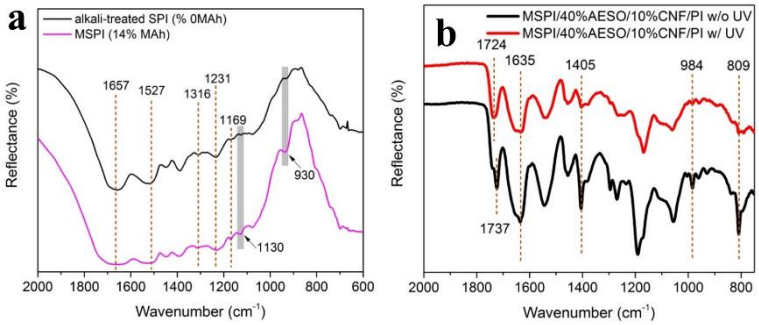

Figure 1. FTIR spectra of alkali-treated SPI and MSPI (a), and uncrosslinked and crosslinked MSPI films (b).

Drug release study of the four aspirin-loaded films was performed in a PBS buffer solution. Each film was kept inside a dialysis tube and immersed in the PBS solution. To prepare a UV-vis sample for aspirin concentration test, a small amount of the solution was drawn from the buffer at predetermined time intervals and the withdrawn solution was replaced with the same amount of fresh solution immediately to keep the volume constant. UV-vis spectrum of the sample solution was obtained and the absorption peak at 275 nm was used to calculate the aspirin concentration in the solution and the cumulative aspirin release from the film at different release time.

The cumulative release of the four films (formulations) within 6 days are compared in Figure 2. Comparing the two formulations using PEGDA as the crosslinker, MSPI/40%PEGDA/10%CNF/PI showed higher drug release rate and amount than MSPI/40%PEGDA/5%CNF/PI. Similarly, when comparing the two formulations using AESO as the crosslinker, MSPI/40%AESO/10%CNF/PI exhibited higher release rate and amount than MSPI/40%AESO/5%CNF/PI. These results indicate that a higher CNF content could result in a faster and greater drug release. This behavior can be attributed to CNF's high affinity toward water, which facilitated the diffusion of PBS solution into the film and accelerated the release. Comparing the formulations containing the same contents of CNF, the ones using PEGDA as the crosslinker showed higher release rate and amount than the ones using AESO. This difference can be ascribed to PEGDA's longer chain and lower functionality than AESO, which led to a lower crosslink density in the films containing PEGDA. The lower crosslink density caused a less dense film structure, which facilitate the diffusion of the PBS solution into the film.

Thermally cured BC/MSPI system

Methacrylation of SPI and crosslinking of MSPI

Grafting of methacrylate groups onto SPI through methacrylic anhydride's reactions with the amine groups on SPI introduced C=C double bond moieties onto SPI (Figure 3a). After being activated by the thermal initiator, the double bonds proceeded to react with each other to connect different SPI chains together through addition polymerization. The successful functionalization of SPI with MAh and its subsequent thermal crosslinking was confirmed by ^{1}H NMR spectra in Figure 3b and photographs in Figures 3c and d. As shown in Figure 1b,

three new peaks appeared atδ=5.5, 5.2, 1.7 ppm in the spectrum of MSPI after the methacrylation. The peaks at 5.5 and 5.2 ppm were assigned to hydrogens on the double bond (A) and the one at 1.7 ppm corresponded to hydrogen of the methyl group (B) of the introduced methacrylate groups. Compared to MSPI, the three peaks of the cured MSPI largely disappeared due to the conversion of $-C(CH_3)=CH_2$ into $-C(CH_3)-CH_2-$ during the thermal crosslinking process. Figures 1c and d show the MSPI solution containing thermal initiator turned into gel after thermal incubation at 100 °C for 6h. During the process, free radicals generated from the added thermal initiator attacked the C=C bonds of the grafted methacrylate groups and induced cross-linking between these groups, leading to covalently crosslinked MSPI hydrogel.

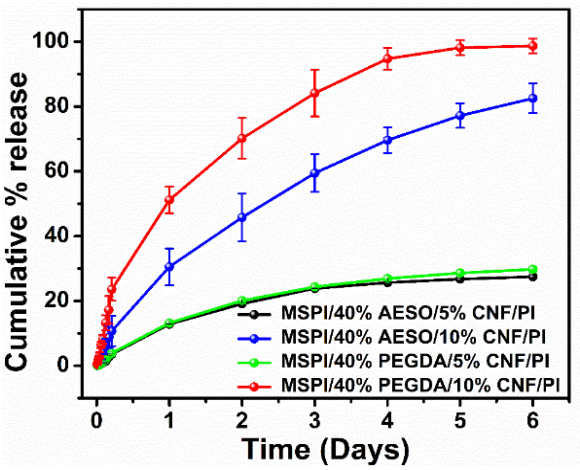

Figure 2. Cumulative aspirin release of MSPI/40%AESO/5%CNF/PI, MSPI/40%AESO/10%CNF/PI, MSPI/40%PEGDA/5%CNF/PI, and MSPI/40%PEGDA/10% CNF/PI films.

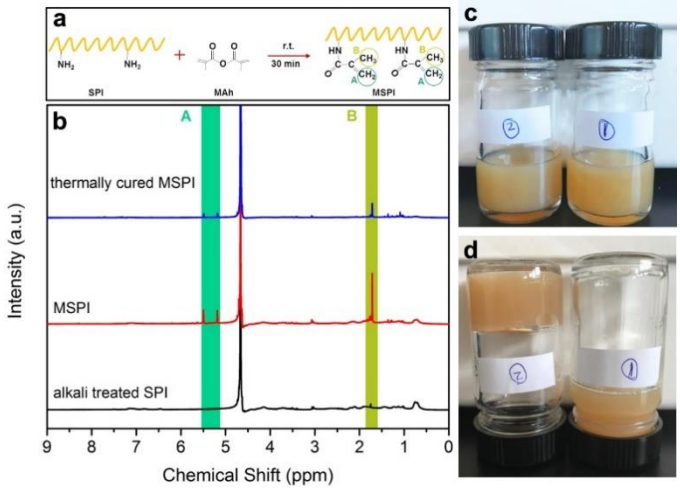

Figure 3. Schematic illustration showing the scheme of MSPI synthesis (a); ^{1}H NMR spectra of alkali treated SPI, MSPI, and thermally cured MSPI (b); photographs of MSPI solution before (c) and after 6h thermal curing at 100 °C (d) (MSPI concentration: 12.15 wt%; in figure c and d, sample 1 contained no thermal initiator while sample 2 contained the initiator).

Formation and Morphology of BC/MSPI composite hydrogels

BC/MSPI composite hydrogels were prepared by crosslinking MSPI solution of different concentrations that was impregnated into BC and the products were freeze-dried. For comparison, pure BC and non-crosslinked BC/8.15%MSPI hydrogels were also freeze-dried using the same drying condition. As shown in Figure 4, the color of BC/MSPI composite hydrogels before curing changed from milky white to light yellow, light brown, and eventually to dark brown as the concentration of MSPI solution was gradually increased from 4.15% to 12.15%. It was found that 4.15% MSPI solution could not undergo crosslinking because the concentration was too low, and the 8.15% MSPI solution could only undergo weak crosslinking to form weak/loose hydrogel network. Comparing BC/MSPI composite hydrogels before and after thermal curing, it is clear that the BC/4.15%MSPI composite hydrogel maintained its light-yellow color and transparency after curing because the absorbed 4.15%MSPI solution could no crosslink and remained in its solution state. By contrast, BC/8.15%MSPI, BC/10%MSPI, and BC/12.15%MSPI lost their transparency and became solid-like because the impregnated MSPI solutions crosslinked and turned into solids. With increasing MSPI concentration, the cured BC/MSPI composite hydrogels became increasingly solid-like/hard.

Morphology of the BC/MSPI composite hydrogels was studied by comparing SEM images of the cross-sections of the gels (Figure 5). Pure BC in Figure 5a exhibits a three-dimensional (3D) nano-fibrillar network structure, which agrees with the typical BC morphology reported by other researchers. Comparing this image with the rest of the images where MSPI was included, it can be found that both the concentration of MSPI and the gel's crosslinking status had impact on the morphology of the gels. Comparing all non-crosslinked gels, with increasing MSPI concentration (5a to 5c), more MSPI can be seen wrapping around BC nanofibers and linking the nanofibers together by forming thin sheets between them. Comparing Figure 5c and 5d (BC/8.15%MSPI), it appears that the crosslinking increased the pore size of the porous structure. Higher MSPI concentrations (10% and 12.15% in 5e and 5f, respectively) led to even larger pore sizes and thicker cavity walls. These morphology changes can be attributed to the movement of MSPI during the crosslinking process, in which MSPI can deform under heat and shrink during crosslinking. A higher concentration of MSPI caused a larger degree of deformation.

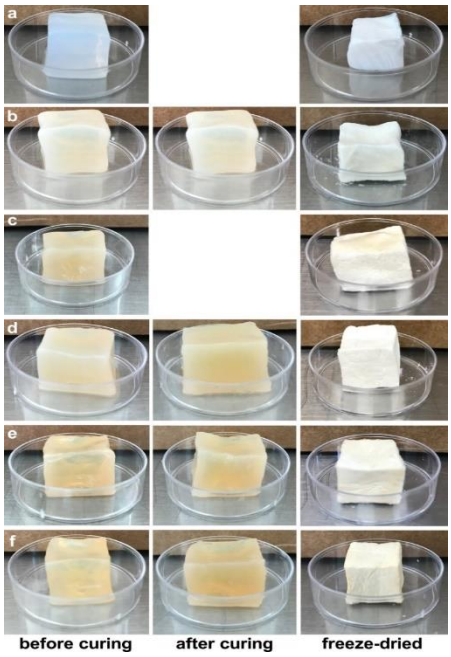

Figure 4. Images of pure BC (a), non-crosslinked BC/8.15% MSPI (b), BC/4.15% MSPI (c), BC/8.15% MSPI (d), BC/10% MSPI (e), and BC/12.15% MSPI (f) composite hydrogels at different processing stages.

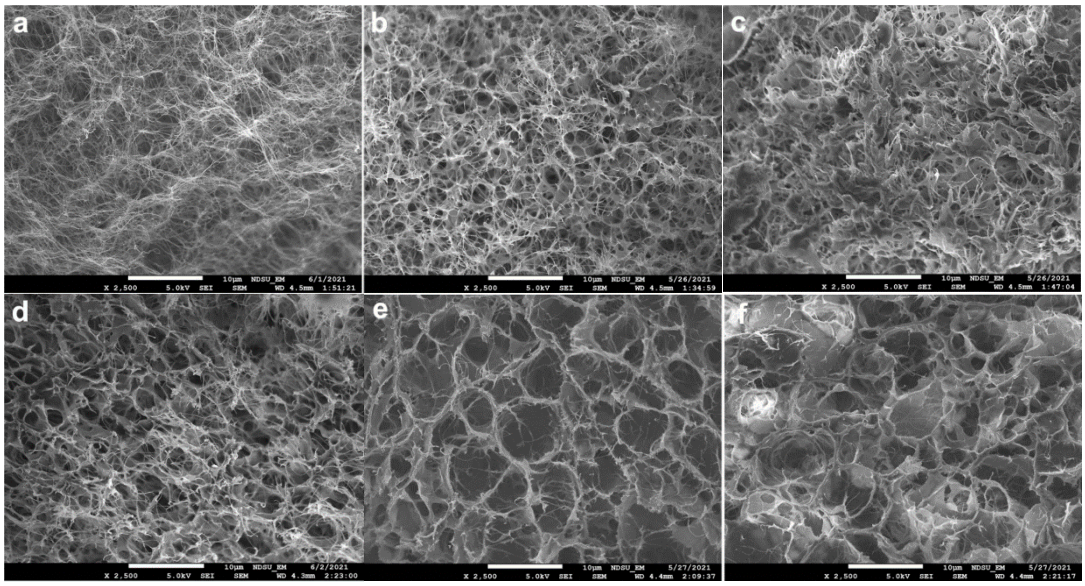

Figure 5. SEM images of the cross-section of freeze-dried BC (a), non-cosslinked BC/4.15%MSPI (b), non-crosslinked BC/8.15%MSPI (c), crosslinked BC/8.15%MSPI (d), crosslinked BC/10%MSPI (e), and crosslinked BC/12.15%MSPI hydrogels (f).

Compressive mechanical properties of BC/MSPI composite hydrogels

Figure 6 shows the compressive stress-strain curves of freeze dryied BC/MSPI hydrogels. Similar to the SEM results, both MSPI concentration and crosslinking status affected the mechanical properties of the gels. The increases in MSPI concentration and the crosslinking led to increased compressive stress and modulus but decreased fracture strain. As shown in Figure

6, pure BC (at the bottom of the figure) showed the highest strain but lowest stress and modulus, exhibiting a nonlinear and viscoelastic behavior typical for soft porous material (Figure 6a). The inclusion of MSPI and its connection between the nanofibers in non-crosslinked BC/4.15%MSPI (shown in Figure 6b) greatly increased gel strength and modulus while maintaining pure BC's high failure strain. A higher MSPI concentration (8.15%) resulted in a further increase in modulus but greatly reduced strength and failure strain of the gel. This behavior can be attributed to the denser, less porous structure of the higher concentraton gel, where MSPI (which is much more brittle compared to the BC network) restrained the movement of the fibers in the gel during the compression.

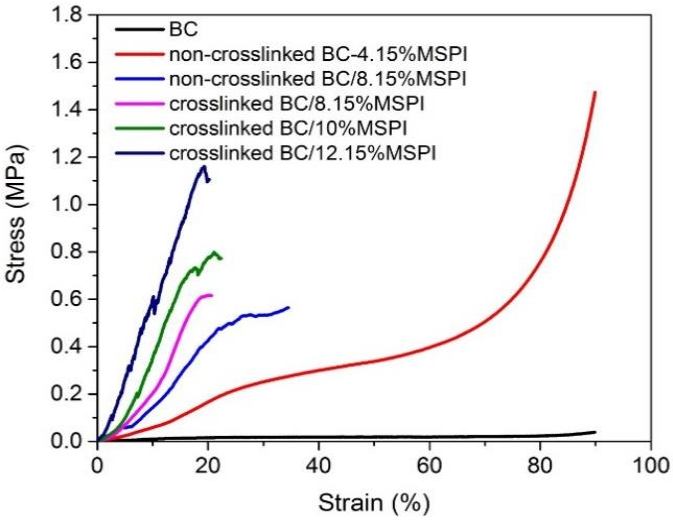

Figure 6. Compressive stress-strain curves of freeze-dried BC/MSPI composite hydrogels.

Crosslinking made MSPI stronger and hardner, which resultantly produce stronger and harder BC/MSPI gel. This can be observed by comparing the BC/8.15%MSPI gel before and after crosslinking in Figure 6. Further increases in MSPI concentration from 8.15% to 10% and 12.15% led to even higher strength and modulus of the gels because MSPI made a greater contribution to the gel properties with its increasing content in the gel.

Water swelling and solubility of BC/MSPI composite hydrogels

The swelling behavior of BC/MSPI composite hydrogels in water is presented in Figure 7a. All samples swelled rapidly during the first 1h, which can be related to the porous structure inside the hydrogels. After that, the swelling slowed down and reached equilibrium within 48 to 72h. Pure BC exhibited the highest swelling ratio of 87.7 because of its high affinity to water molecules and 3D nano-fibrillar network with large number of pores, which resulted in high water permeability and high water holding capacity. The swelling ratio was significantly decreased after the incorporation of 4.15% MSPI, with the value being decreased to 14.7 for the non-crosslinked BC/4.15%MSPI. Higher MSPI concentrations and crosslinking led to further decreases in sample swelling. The swelling ratio of 9.26, 9.69, 9.14, and 7.68 was achieved for non-crosslinked BC/8.15%MSPI, crosslinked BC/8.15%MSPI, crosslinked BC/10%MSPI, and crosslinked BC/12.15%MSPI, respectively. The decreases are due to the reduced porosity and increased hydrophobicity of the gel as well as enhanced constraints on the movement of the nanofibers by the crosslinked MSPI.

The solubility of BC/MSPI composite hydrogels in water is presented in Figure 7b. Pure BC shows the highest water resistance with no weight loss observed because its highly crystalline cellulose nanofibers are completely insoluble in water. On the other hand, uncrosslinked BC/4.15%MSPI and BC/8.15%MSPI showed the highest water solubility among all the fabricated hydrogels, with only 17.3% residual mass for the former and 18.8% for the latter. The mass loss is mainly due to the dissolution and release of the uncrosslinked MSPI from the BC fiber network. SPI still exhibited hydrophilicity and water solubility even after methacrylation, which made MSPI soluble in an aqueous solution. However, crosslinked BC/MSPI composite hydrogels showed markedly improved water resistance. The remaining mass increased to 31.1% for crosslinked BC/8.15%MSPI and 83.4% for crosslinked BC/12.15%MSPI, indicating that crosslinking significantly reduced the solution of MSPI.

Fertilizer release

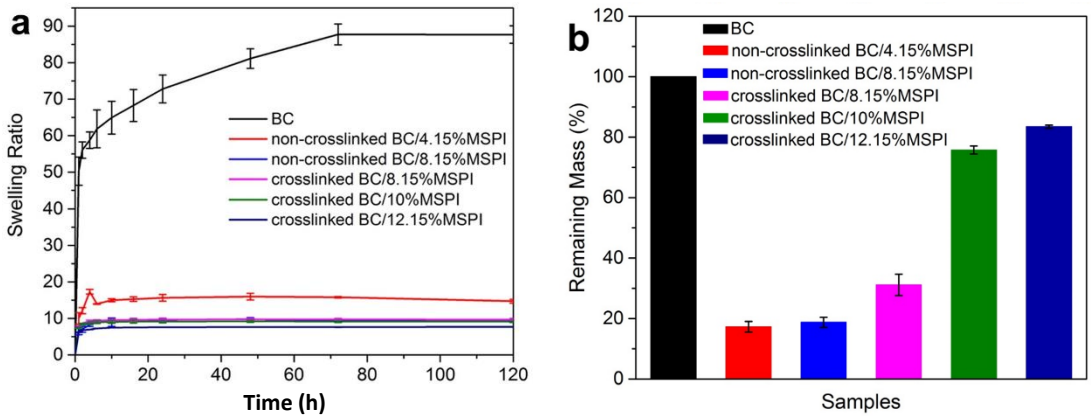

Figure 7. Swelling ratio as a function of time (a) and water solubility (b) of BC/MSPI composite hydrogels.

The $(NH_4)_2SO_4$ release profiles for all the samples measured by the conductivity tests are shown in Figure 8. Freeze-dried MSPI hydrogel containing no BC did not show a sustained release as the non-crosslinked 8.15%MSPI gel demonstrated an almost immediate, complete release due to rapid dissolution of MSPI in water. Crosslinked 8.15%MSPI showed a slight delay in release (plateaued 30min later than the non-crosslinked) as the gel disintegrated into big chunks rather than dissolved in water.

Sustained release of $(NH_4)_2SO_4$ can be observed from the BC/MSPI gels where BC was incorporated to reinforce/stabilize the gel structure. Non-crosslinked BC/4.15%MSPI, non-crosslinked BC/8.15%MSPI, and crosslinked BC/8.15%MSPI composite gels showed release rates similar to that of pure BC, reaching the equilibrium within 5 h. Further controlled release can be observed for crosslinked BC/10%MSPI and crosslinked BC/12.15%MSPI, with their equilibrium being reached within 16h. These results correspond well with the swelling and dissolution results of the gels. The gels containing high content, crosslinked MSPI possesses stronger water resistance and a lower solubility, making the fertilizer harder to dissolve and diffuse into the water and therefore providing more sustained release.

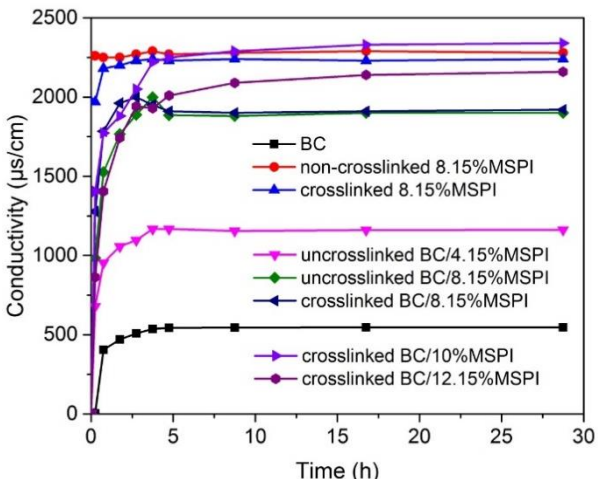

Figure 8. Fertilizer release indicated by water conductivity at 25 ◦C.

It should be pointed out that although the conductivity of the solution can indicate fertilizer content in the solution, it does not represent the accurate fertilizer content because other charged particles (e.g., dissolved MSPI and residual chemicals from SPI treatments) released into the solution can also increase its conductivity. Nevertheless, their contributions are relatively small and are not expected to affect the trend/shape of the release profiles.

Conclusion

In this project two soy protein-based controlled chemical delivery systems were developed by using UV and thermal curing respectively. The UV system was easier/faster to fabricate at a lower cost than the thermal system. It also appears that the former provided more sustained chemical release in water. The actual release in soil is expected to be even more sustained because the water content of soil is relatively low. More systematic studies on both systems are desired to determine the optimal formulations and processing conditions tailored for specific release requirements.